REVIEW

National Science Review
4: 91–105, 2017
doi: 10.1093/nsr/nww098
Advance access publication 7 January 2017

MATERIALS SCIENCE

Special Topic: Energy Storage Materials

Progress and directions in low-cost redox-flow batteries for large-scale energy storage

Bin Li* and Jun Liu*

ABSTRACT

Compared to lithium-ion batteries, redox-flow batteries have attracted widespread attention for long-duration, large-scale energy-storage applications. This review focuses on current and future directions to address one of the most significant challenges in energy storage: reducing the cost of redox-flow battery systems. A high priority is developing aqueous systems with low-cost materials and high-solubility redox chemistries. Highly water-soluble inorganic redox couples are important for developing technologies that can provide high energy densities and low-cost storage. There is also great potential to rationally design organic redox molecules and fine-tune their properties for both aqueous and non-aqueous systems. While many new concepts begin to blur the boundary between traditional batteries and redox-flow batteries, breakthroughs in identifying/developing membranes and separators and in controlling side reactions on electrode surfaces also are needed.

Keywords: redox-flow batteries, energy storage, large scale, cost, electrolytes

Pacific Northwest National Laboratory, Richland, WA 99352, USA

*Corresponding authors. E-mails: bin.li@pnnl.gov; jun.liu@pnnl.gov

Received 31 October 2016; **Revised** 9 December 2016; **Accepted** 3 January 2017

INTRODUCTION TO ENERGY STORAGE AND BATTERIES

Energy storage is a key technology that is becoming more and more important in the energy infrastructure. Currently, approximately 30% of energy consumption is in the transportation sector, and 40% of that use is in the form of electricity [1]. The increasing supply of electrical energy from renewable resources causes great concerns for the performance and reliability of the electrical grid infrastructure. It is predicted that by 2020, renewable wind and solar resources will supply 12% of electricity in the USA and 20% in Europe [2]. Electrical-energy storage is a powerful tool for improving the flexibility of integrating renewable energy into the grid, improving grid reliability, increasing the use of renewable resources, extending the service life of the infrastructure and improving power quality.

Rechargeable batteries have many applications. As displayed in Fig. 1a [3], a battery is normally made of a cathode and an anode material immersed in an electrolyte. Energy is stored in the electrode materials. Ions are shuttled between the cathode and anode through the electrolyte, while electrons are transported as electrical current through external circuits. Rechargeable secondary batteries are commonly made of solid-state cathode and anode materials. These include lithium-ion (Li-ion) batteries, lead-acid batteries, sodium-sulfur batteries, nickel-cadmium batteries, etc. [4,5]. Currently, because of its low cost and wide-ranging applications, the lead-acid battery is the most extensively used technology in the marketplace [6]. However, lead-acid battery technology is limited by shallow charge–discharge capacity, short cycle life and the use of hazardous lead. Li-ion and redox-flow batteries (RFBs) are the two main technologies currently competing with lead-acid battery for future applications. Although there have been many excellent reviews on RFBs, there are still doubts regarding the future of this technology when compared to Li-ion batteries, and questions remain regarding breakthroughs needed to enable large-scale deployment of RFBs.

RFBs

Batteries can be made with a range of solid and liquid electrode material combinations (Fig. 2). In an

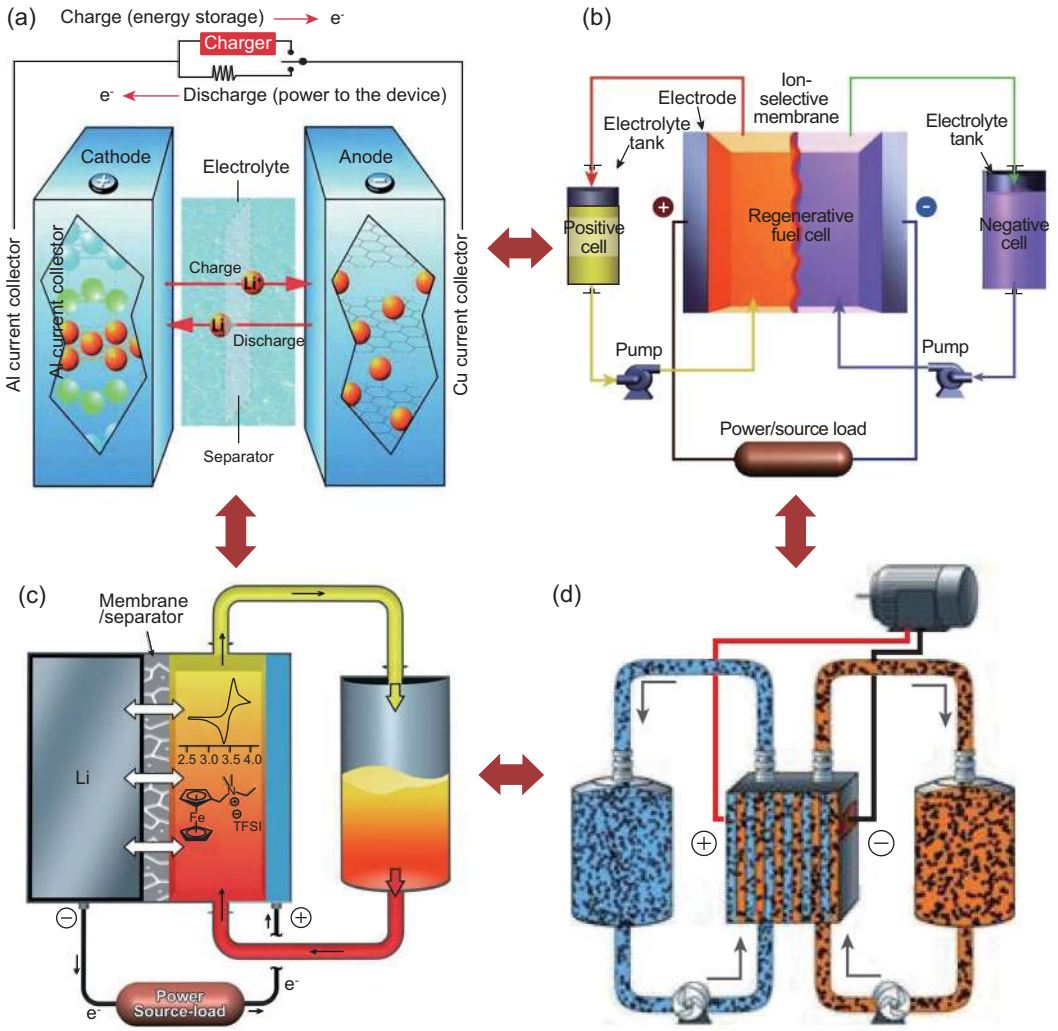

Figure 1. Schematic of different configurations of electrode materials in batteries. (a) Traditional Li-ion battery made of solid electrode materials [3] (Copyright 2014 Royal Society of Chemistry). (b) Redox-flow batteries in which the electrode materials are made of liquids [12] (Copyright 2011 Wiley). (c) A hybrid battery, in which half the cell is made of liquid electrolyte, and half is made of solid electrode material [36] (Copyright 2015 Wiley). (d) A semi-solid battery in which the active materials are dispersed in electrolytes [87] (Copyright 2011 Wiley).

RFB, the cathode and anode materials are made of electrolyte solutions (i.e. catholytes and anolytes) in which the energy is stored. As shown in Fig. 2b [7], electrolyte at the anode and cathode sides is pumped through porous electrodes located at each side in a cell stack, where they are separated by an ion-exchange membrane or porous separator to prevent mixing. Electrochemical redox reactions occur on the electrode surfaces. This unique architecture of RFBs allows independent scaling of the power and/or energy. The power is defined by the size and design of the electrochemical cell (the stack) whereas the energy depends on the amount of stored electrolyte. The energy to power ratio (E/P) can be varied over a wide range. A high E/P ratio can reduce the cost of the whole system by more than 50% on an energy basis [8]. On the other hand, because they are particularly well suited for small- and intermediate-scale applications and for short-term duration and fast response times, Li-ion batteries are well positioned for applications in the electronics and automobile industries. However, scaling up Li-ion batteries is difficult and requires additional management systems for small-format battery cells [9–12].

There are many scientific and technological challenges, including cost, reliability and safety, equitable regulatory environments and industry acceptance, for large-scale deployment [13]. Data in the open literature suggest that most battery technologies still cost over $500/kWh [14,15]. The

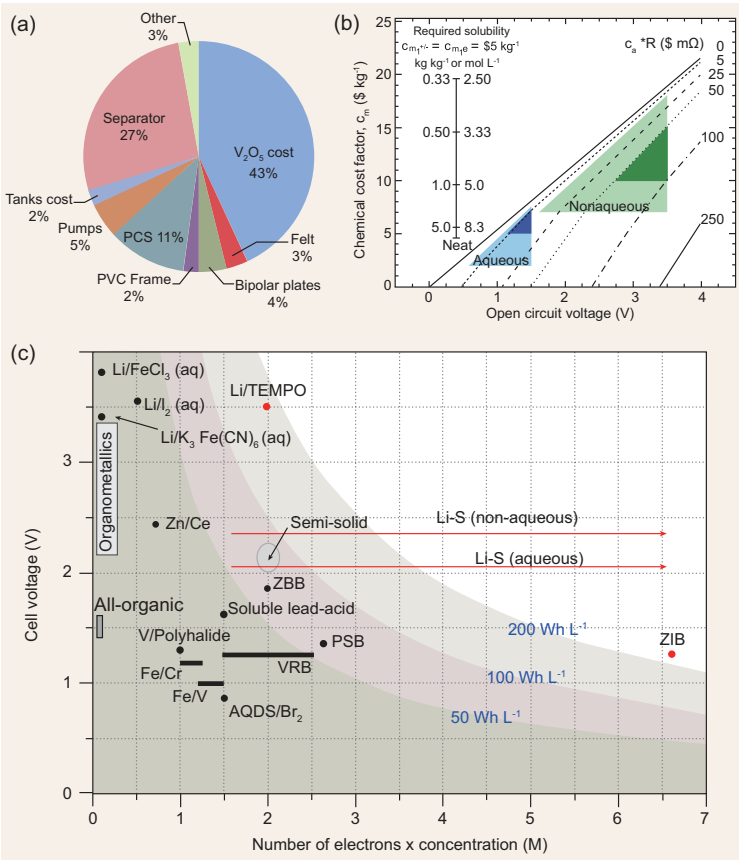

Figure 2. (a) Distribution of costs for 4-MWh mixed-acid VRB [8] (Copyright 2014 Elsevier). (b) Allowable chemical cost factor on an active species basis (in $/kg) vs. OCV for a range of reactor costs (caR in $mΩ). All points on a line give a system price of $120 per kWh. The region U < 1.5 V is considered to be available to aqueous systems. The dark-shaded triangles are considered to have a higher likelihood of achievability compared to the larger lighter-shaded triangles. The leftmost inset vertical scale shows the required solubility (in kg/kg) of a non-aqueous active species when solvent and solute cost $5/kg. The rightmost inset vertical scale on the right shows the molar concentration, assuming specific volumes of 1 L/kg [11] (Copyright 2014 Royal Society of Chemistry). (c) Summary of the reported cell voltages, effective molarities and energy densities of various aqueous and non-aqueous RFBs [19] (Copyright 2014 Wiley).

capital cost target needs to be close to $100/kWh to compete with the cost of electricity in the USA [11]. The US Department of Energy (DOE)'s Advanced Research Projects Agency—Energy has established a capital cost target of $100/kWh for one hour of storage for widespread adoption [16]. The DOE's Office of Electricity Delivery and Energy Reliability proposed a cost target of $250/kWh to be achieved by 2015, and decreasing to $150/kWh in the future for fully integrated distributed energy-storage systems providing four hours of storage [17].

The cost of an RFB is determined by the active redox materials, the supporting electrolyte, the stack (which includes the electrodes, membranes, frames, and bipolar and end plates) and the accessory components (pumps, plumbing, etc.) [8,18]. In addition to the cost of raw materials, Fig. 1a shows an example of the cost breakdown of a typical 4 MWh vanadium RFB (VRB) [8]. Clearly, the cost of the active material is significant. Gallagher *et al.* [11] analysed the cost and performance of various redox chemistries. As shown in Fig. 1b, both non-aqueous and aqueous flow batteries have the potential to be produced for $120/kWh. The chemical cost factor (c_m, $/kg) is determined by the costs of active materials, salts, solvents and storage vessels. The factor of c_aR represents the reactor (stack) cost. From Fig. 1b, to meet a cost target of $120/kWh, a lower chemical cost is required with decreasing open circuit voltage (OCV) or increasing reactor cost. The required chemical costs for an aqueous system is much lower than that for non-aqueous systems because of a lower OCV. The cost of active species in non-aqueous and aqueous systems should be less than $19/kg and $8/kg, respectively. Non-aqueous electrolytes should be no greater than $5/kg, and aqueous electrolytes must be almost free. The solubility of active materials in aqueous systems and non-aqueous systems should reach 5 M and more than 2 M, respectively. Obviously, one approach for reducing the cost is to use inexpensive active redox materials, the supporting electrolyte and stack materials. The cost also can be reduced by performance optimization of flow batteries. For example, increasing the conductivity of membranes and kinetics of electrode toward a redox reaction in electrolytes would decrease cell overpotentials, which suggests the required stack size could be reduced for an equivalent power output (i.e. power density). The increase in energy density for a flow battery system suggests that the footprint cost could be reduced because the energy is stored in anolytes and catholytes inside tanks. In addition, system costs can be reduced by simplifying manufacturing and management requirements. Finally, improved reliability of flow battery systems, which is determined by the chemical stability of electrolytes, membranes, electrodes, etc., would significantly contribute to increased battery service life, thus greatly reducing the life cycle costs.

So far, a wide range of redox-flow chemistry systems have been studied. Figure 1c shows that energy density is a function of concentration and cell voltage for different flow battery systems [19]. As seen in Fig. 1c, lithium/sulfur (Li/S) and zinc-polyiodide (ZIB) battery systems exhibit the highest energy densities because of the high solubility of the active materials. Non-aqueous RFBs, such as organometallics and all-organic systems, show lower energy densities than most aqueous RFBs because of the lower solubility of active species, although the cell voltages of these systems are higher. While more detailed discussions will be provided for selected

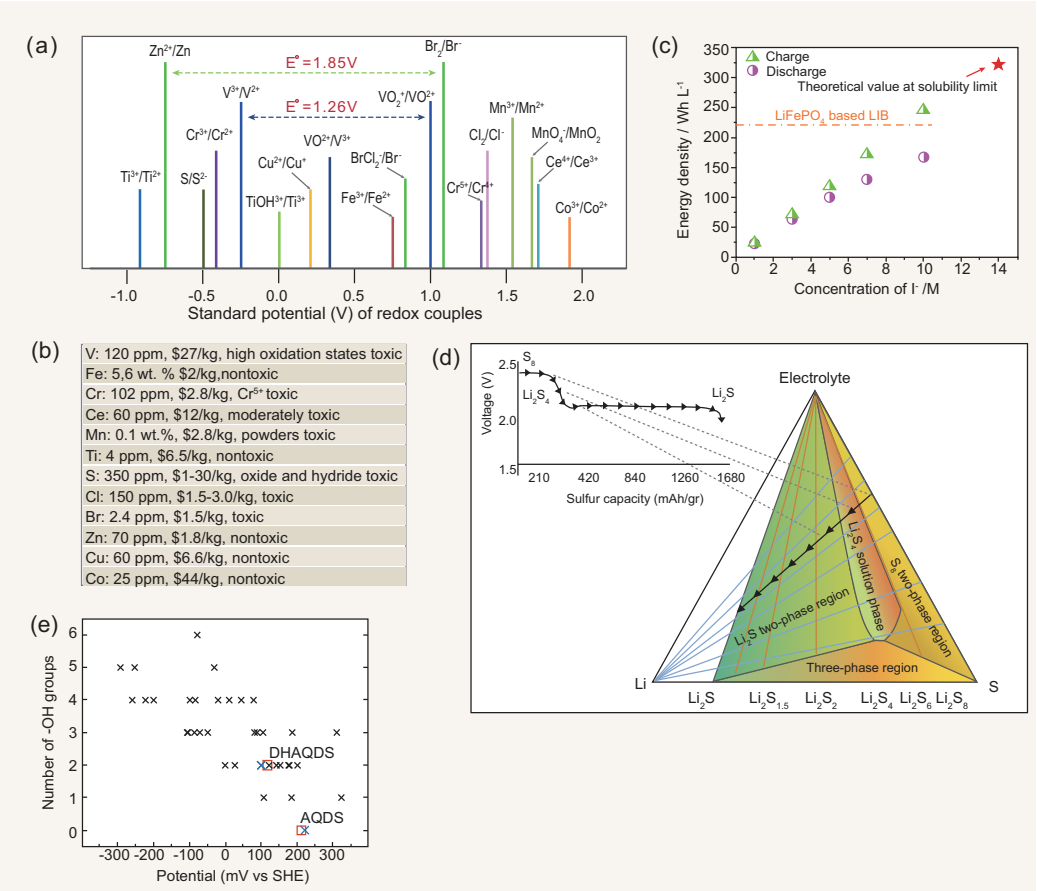

Figure 3. (a) Redox potential of various inorganic redox couples [22] (Copyright 2011 American Chemical Society). (b) The cost of active species displayed in (a). (c) The charge and discharge energy densities as a function of the concentration of I^- [37] (Copyright 2015 NPG). (d) Ternary phase diagrams of Li_xS_y. (e) Calculated reduction potentials of AQDS substituted with –OH groups (black), calculated AQDS and DHAQDS values (blue), and experimental values for AQDS and DHAQDS (red squares) [51] (Copyright 2014 NPG).

redox chemistries, most redox materials are too expensive and have solubility far below the required levels needed to attain cost targets.

AQUEOUS REDOX-FLOW CHEMISTRY

Because of good safety characteristics and high power densities (e.g. VRBs and hydrogen/bromine RFBs) [20,21], aqueous systems have attracted widespread interest. One of the disadvantages is the lower energy density. Figure 3a shows the potentials of traditional redox couples made of inorganic materials [22]. The availabilities, toxicities and approximate costs of the materials are listed in Fig. 3b. From these results, most of the materials are still too expensive within the stability window of water. The most widely studied redox species, vanadium, is expensive and toxic in its oxidized form. Ideally, low-cost, environmentally friendly species made of iron, zinc, manganese or sulfur could be used. There has been great interest in completely or partially replacing vanadium with iron and chromium [23,24]. However, hydrogen forms at the anodes of the iron/chromium (Fe/Cr) RFBs [25] and expensive vanadium is used at both sides in iron/vanadium (Fe/V) RFBs to minimize crossover contamination [24,26].

Vanadium flow battery

Since 1986 [27], VRBs have been widely investigated because electrolytes on both anode and cathode sides use vanadium species to minimize crossover contamination. Sulfuric acid has been used as supporting electrolytes. While the traditional VRB system was first scaled up to 250 kW/2 MWh for demonstration in the USA in 2004, there is still a concern about the high cost, low solubility and precipitation of V_2O_5 over a wide temperature range [28]. The low solubility of vanadium ions (<1.7 M) limits the system to a low energy density of 25 Wh/L

[29–31]. The potential for precipitation of V_2O_5 in the catholyte when electrolyte temperature exceeds 40°C for an extended period of time may reduce reliability and battery life. Recently, a mixed-acid VRB system was reported, in which chloride ions were added to vary the solvation structure of vanadium ions in the solution, thus increasing the solubility to over 2.5 M. The energy density of mixed-acid VRB was increased by more than 70% relative to traditional VRB while expanding the temperature operation window by 80% [7]. The mixed-acid system has been successfully scaled up and is commercially produced [32]. Still, as mentioned earlier, vanadium is expensive. The ultimate solution is to find highly soluble, low-cost redox materials for aqueous systems. In addition, in VRBs, perfluorosulfonic acid ionomer (Nafion) membranes are used [33–35]. Nafion membranes consist of a perfluorinated backbone with pendant vinyl ether side chains terminated with sulfonic acid (SO_3H) groups. The ion conductivity is limited, not selective enough and degrades over time. It also happens to be the second most expensive component in the system [8]. Capacity fading originating from active-ion crossover might not be avoided because of the poor ion selectivity or the chemical instability of the membranes. To retard capacity fading, chemically stable and highly ion-selective membranes are required.

Hybrid flow battery systems

In traditional RFB systems, such as VRBs and Fe/Cr RFBs, energy-density calculations include two liquid electrolytes on both sides (Fig. 2b). However, as shown in Fig. 2c [36], for a hybrid flow battery design, energy density is determined only by the liquid volume on one side. In this design, one half-cell features a solid electrode and the electrolyte possesses ambipolar and bifunctional characteristics. In such electrolytes, cationic and anionic ions from a single soluble compound are both energy-bearing redox-active species, thus eliminating the need for non-active counter ions such as Cl^- and SO_4^{2-} that are commonly used in VRB and Fe/Cr RFB systems. This design minimizes the amount of electrolyte in one half-cell and achieves a high active species concentration in the other half-cell [37]. The traditional aqueous zinc/bromine RFB (ZBR) [38], ZIB RFB [37] and Li metal-based hybrid flow battery that are discussed below all follow the above design strategies.

When ZBR systems are being charged, zinc metal is plated on the anode side of a carbon-based electrode. Meanwhile, bromide ions (Br^-) are oxidized to bromine (Br_2) at the cathode side. During discharge, the reverse process occurs [39]. This system has a high cell voltage and energy density, and expectations are that low-cost materials can be used. However, demonstration of ZBR systems has been limited because of material corrosion, dendrite formation and electrical shorting, high self-discharge rates, low energy efficiencies and short cycle life. The existence of corrosive bromine at the cathode side is the cause of some of these problems. Expensive cell electrodes, membranes and fluid-handling components are needed to withstand the chemical conditions. In addition, bromine has limited solubility in water and is toxic. Therefore, it is critical that organic agents be used to complex the bromine to mitigate the crossover contamination and toxicity of bromine when it sinks to the bottom of the catholyte tank. In 2014, Li *et al.* reported a new environmentally friendly flow battery system [37]. They developed a novel ZIB system in which bromine was replaced with soluble I_3^-/I^- redox couples. A high energy density of 167 Wh/L, which approaches that of Li-ion batteries, is achievable (Fig. 3c) based on the high solubility of zinc iodide electroytes (>7 M). The ambipolar and bifunctional designs of the ZIB use zinc ions as both the redox-active species and charge carriers, eliminating the need for non-active counter ions. Together with the high selectivity of the Nafion membrane against iodide anions, the ZIB system delivers a very high coulombic efficiency (CE) value (~99%). The energy efficiency (EE) values decrease from 90.9% to 76.0% as the concentration of ZnI_2 increases from 0.5 to 3.5 M when operated at a current density of 20 mA/cm^2. The cell shows excellent cycling performance. Figure 4a shows the typical charge/discharge curves at 1.5 M ZnI_2. The addition of an alcohol (ethanol) induces ligand formation between oxygen on the hydroxyl group and the zinc ions, which expands the stable liquid electrolyte temperature range from –20°C to 50°C. As we know, dendrite growth is one of the issues to be addressed for most metal anode-based batteries, such as Zn- and Li-based systems, which would cause serious short-circuit and safety concerns. Here, the addition of an alcohol was found to effectively ameliorate the zinc dendrite propagation.

Aqueous lithium flow battery

The similar metal anode concept has been investigated in Li flow systems. Taking advantage of the high solubility and low viscosity of aqueous solutions and the low potential of Li/Li^+, Goodenough's group [40] and Zhou's group [41] proposed a cell that uses Li metal with a non-aqueous electrolyte at the anode side and

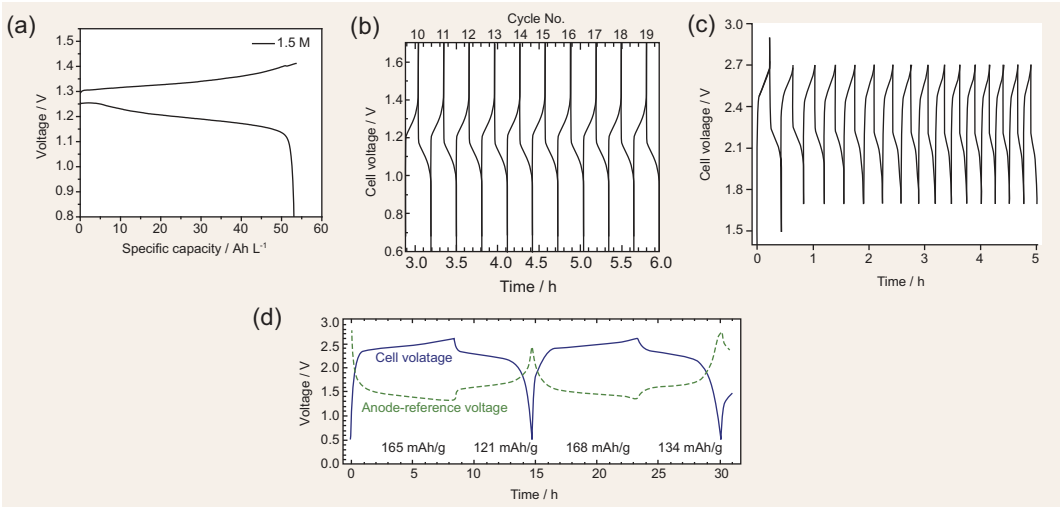

Figure 4. (a) Typical charge/discharge curves for ZIB systems at 1.5 M ZnI_2 [37] (Copyright 2015 NPG). (b) Representative voltage versus time curves during 100 charge–discharge cycles at 100 mA/cm^2, recorded between the 10th and 19th cycles [56] (Copyright 2015 AAAS). (c) Typical cycling voltage curves of the flow cell using 0.5 M FL/0.5 M DMBBM/1.0 M TEA–TFSI/MeCN at 15 mA/cm^2 [76] (Copyright 2015 Wiley). (d) Two iterations of injection and galvanostatic cycling for a full lithium-ion flow cell operating between 0.5 and 2.6 V at C/8 rate. Suspensions are 20 vol% $LiCoO_2$, 1.5 vol% Ketjen black and 10 vol% $Li_4Ti_5O_{12}$, 2 vol% Ketjen black, both in 1 M $LiPF_6$ in dimethyl carbonate [87] (Copyright 2011 Wiley).

aqueous solutions as the catholytes on the other side. To prevent the reaction of Li metal and water, a dense solid electrolyte separator (e.g. LISICON: $Li_{1+x+3z}Al_x(Ti,Ge)_{2-x}Si_{3z}P_{3-z}O_{12}$) with high Li-ion conductivity is a critical component of this configuration.

Investigations of Li systems have led to high interest in the use of sulfur, which is widely available and very inexpensive compared to other materials. The high solubility of polysulfide species also could also lead to battery systems that possess high energy densities (Table 1). Figure 3d shows ternary phase diagrams of Li_xS_y. The theoretical sulfur capacity can be as high as 1672 mAh/g. Cui's group [42] and Liu's group [43] studied rechargeable redox-flow Li-S cells using traditional non-aqueous electrolytes. However, a critical problem in the liquid cell is precipitation of short-chain lithium sulfides. An interesting approach was developed by Zhou *et al.* [44] and Visco *et al.* [45,46]. Both groups proposed aqueous lithium–polysulfide batteries, which are based on a short-chain lithium sulfides (Li_2S_4–Li_2S) redox reaction. In this system, a Li-ion conductive glass separator (LATP: $Li_{1.35}Ti_{1.75}Al_{0.25}P_{2.7}Si_{0.3}O_{12}$) isolates the Li metal and aqueous polysulfide electrolytes. The battery shows an OCV of approximately 2.67 V. The unique advantages of aqueous lithium–polysulfide batteries are that the Li_2S_4–Li_2S redox couple possesses high solubility (over 5.0 M [46,47] in the aqueous electrolyte, leading to a high energy density of 387 Wh/L. The LATP separator impedes the polysulfide shuttle during cycling and prevents lithium dendrite growth. However, the reduction of Ti^{IV} in the separators (i.e. LATP or LISICON) at low potential (<1.6 V vs. Li^+/Li) makes it unstable when in direct contact with metallic Li. Therefore, a buffer layer is required to separate the glass ceramic from Li during long-term operation.

Other inorganic materials, such as $FeCl_3$ [41], $K_3Fe(CN)_6$ [48], LiI [49] and LiBr [50], can reach a high concentration in water and were also studied for use as the cathode materials. The corresponding cells all demonstrated good cycling performance (except for $FeCl_3$, which has a low pH), high cell voltage (>2.5 V) and high energy density. However, the low conductivity of the solid electrolyte separator ($\sim 10^{-4}$ S/cm vs. 0.1 S/cm for Nafion) produced a smaller operating current density and, therefore, a lower power output.

Organic flow battery

Although inorganic redox materials have attracted widespread attention, organic redox materials can offer more flexibility to tune the redox activity, solubility and stability. In 2014, the Aziz group [51] and Narayanan group [52] proposed the use of a water-soluble, metal-free organic redox couple (i.e. quinone-based) in RFBs. Quinone derivatives are attractive because of their low cost ($5–$10/kg vs. $27/kg for vanadium) and their availability from biological processes.

Table 1. Calculation of energy density of Li–S flow batteries with different sulfur concentrations.

		$S_8^{2-} \rightarrow S_4^{2-}$	$S_8^{2-} \rightarrow S_2^{2-}$	$S_8^{0} \rightarrow S_4^{2-}$	$S_8^{0} \rightarrow S_2^{2-}$	$S_8^{0} \rightarrow S^{2-}$
Capacity (mAh/g)		209	627	418	836	1672
Voltage (V)		2.2	2	2.2	2	2
Energy (weight) density (Wh/kg)		459	1254	919	1672	3344
Volumetric energy density (Wh/L)	0.5M	7	20	14	26	53
	1M	14	40	29	53	106
	2M	29	80	58	107	213
	5M	73	125	147	214	534
	10M	146	250	294	428	1068

The Aziz group chose 9,10-anthraquinone-2,7-disulfonic acid (AQDS) and bromine as anode active material and cathode active materials, respectively, which revealed a high rate of 7.2×10^{-3} cm/s for two-electron reduction of AQDS to $AQDSH_2$ on a carbon electrode surface. The cell was cycled for 50 cycles with an OCV of 0.8 V and approximately 99% capacity retention per cycle. It also demonstrated 0.6 W/cm^2 at 1.3 A/cm^2. Recently, the power output of quinone-bromine RFBs was increased to 1 W/cm^2 at 4 A/cm^2 [53]. Crossover of bromine or bromide ions and decomposition of quinone molecules contributed to capacity loss [54]. Density function theory calculations showed a strong dependence of the standard potential on the position and number of hydroxyl groups (Fig. 3e). Aspuru-Guzik *et al.* also introduced a high-throughput computational screening approach to study 1710 quinone and hydroquinone redox couples to identify promising candidates [55]. They found that the class of 9,10-anthraquinones (AQ) is a suitable target for the negative side whereas the classes of 1,2-benzoquinones (BQ), 2,3-naphthoquinone and 2,3-AQs are more appropriate for the positive side. Using electron-donating groups (–OH and $–NH_2$) and electron-withdrawing groups ($–SO_3H$, $–PO_3H_2$ and $–NO_2$) can decrease and increase the stand potential. Moreover, the effects of these groups (electron-donating or electron-withdrawing groups) on varying the stand potential are increased when these groups are positioned close to the quinone ketone groups.

On the basis of the above predictions, Aziz *et al.* developed the alkaline quinine flow battery [56]. In the alkaline solution, the –OH groups are deprotonated to increase the solubility and good electron-donation capability, which results in an increase in the OCV of 47% over the previously reported system. At the negative side, tuning the pH could shift the thermodynamic potentials of proton-dependent reactions to more negative values. At the positive side, they replaced bromine with the nontoxic ferricyanide ion. Figure 4b shows the representative charge/discharge curves at 100 mA/cm^2 for these systems. Flow cells with 0.5 M 2,6-DHAQ dipotassium salt dissolved in 1 M KOH at the negative side and 0.4 M $K_4Fe(CN)_6$ dissolved in 1 M KOH at the positive side can achieve power densities > 0.45 W/cm^2 at room temperature and 0.7 W/cm^2 at 45°C. Recently, Aziz *et al.* used a water-soluble organic compound, alloxazine, which is a tautomer of the isoalloxazine backbone of vitamin B2, to replace quinone-based compounds at the negative side. The alkaline-soluble allooxazine 7/8-carboxylic acid produces an RFB with an OCV approaching 1.2 V and CE and capacity retention exceeding 99.7% and 99.98% per cycle, respectively. Structural modifications of alloxazine with electron-donating groups are calculated to be able to further increase the battery voltage [57].

The Narayanan group presented all-quinone-based RFB [52]. A solution of 1,2-benzoquinone-3,5-disulfonic acid (BQDS) and a solution of anthraquinone-2-sulfonic acid (AQS) acted as catholytes and anolytes, respectively. The cells did not show noticeable changes in capacity over at least 12 cycles. However, the standard potentials of BQDS and AQS redox couples are 0.85 V and 0.09 V, respectively, leading to a low OCV.

One obstacle in aqueous quinone-based RFB is the low water solubility of quinones. The aqueous solubility limits of BQDS, AQDS, AQS and AQDH (in 1 M KOH) are 1.7 M, 0.5 M, 0.2 M and 0.6 M, respectively. Choosing a substituent to modify quinone-based molecules appears to be one of the most promising approaches to overcome the solubility challenge. The investigations of Aspuru-Guzik *et al.* suggested substitutions of hydrophilic groups such as –OH, $–NH_2$, –COOH, $–SO_3H$ and $–PO_3H_2$ could increase the solubility. Moreover, full substitutions are more useful than single substitutions in improving solubility in water. Functionalization away from the ketone group provides molecules with the highest solubility [55].

The results on quinone systems also suggest that other water-soluble organic molecules

should be studied, particularly those that can be produced from natural products. For example, Liu *et al.* investigated an aqueous organic flow battery using methyl viologen as the anolyte and 4-hydroxy-2,2,6,6-tetramethylpiperidin-1-oxyl (4-HO-TEMPO) as the catholyte [58]. The OCV is 1.25 V, which is similar to that of the VRB. Both organic compounds are highly soluble in water, with solubility over 2 M. The use of an anion-exchange membrane significantly reduces crossover of the cationic redox species, leading to high cycling stability. Similar studies were performed by Schubert's group [59].

NON-AQUEOUS RFBs

In aqueous RFBs, the cell potential is constrained by water electrolysis. Therefore, some recent efforts have shifted to developing non-aqueous RFBs because of the potential to achieve high energy densities due to their wider electrochemical windows. Current non-aqueous RFB research is primarily focused on finding viable redox materials for various flow chemistries, such as metal-ligand complexes and organic redox molecules. Figure 5a shows the redox potentials (vs. Li/Li^+) of representative redox-active organic and organometallic compounds [60]. The organic and organometallic compounds have a wide potential window in the range of 0.7–4 V. The redox potential (vs. Li/Li^+) of promising candidates used as anode and cathode materials should be lower than 2 V and close to or higher than 4 V, respectively, to achieve high cell voltage (>2 V). Some of the organic materials in Fig. 5a, with proper modifications to tailor redox potential, solubility and electrochemical activity, have potential for non-aqueous RFBs.

Organometallic flow battery

The first study of an RFB with a metal-ligand complex ($[Ru(bpy)_3]^{2+}$) was performed by Matsuda *et al.* [61]. This flow chemistry exhibited an OCV of 2.6 V and low efficiency of 40%. Thereafter, other metal-ligand (with the metals being Ru, V, Cr, Mn, Fe and Co, and the ligands being bpy, acac, acacen, phen, mnt) non-aqueous RFBs were studied [62–69]. However, most metal-ligand, non-aqueous RFBs suffer from low CE due to chemical degradation of the redox molecules and poor solubility. To date, the most soluble transition-metal complexes examined for non-aqueous RFB applications involving multiple electron transfers reach saturation at 0.8 M in acetonitrile. Single-electron transfer complexes reach 1.8 M in carbonate solvents. Their energy densities are much lower than those of aqueous systems, although cell potential is larger (>2.0 V). The complicated synthetic procedures, the inherent low solubility and poor chemical stability of metal-ligand complexes have gradually shifted the attention of the research community to all-organic redox molecules.

All-organic flow battery

All-organic flow batteries can take advantage of wide structural diversity and availability of redox molecules from natural abundant resources. The first all-organic RFB was built by Li *et al.*, which used 2,2,6,6,-teramethyl-1-piperidinylxy (TEMPO) and N-methylphthalimide in acetonitrile as catholytes and anolytes, respectively [70]. $NaClO_4$ was added as a conductive salt. Brushett *et al.* at Argonne National Laboratory (ANL) proposed another all-organic, non-aqueous RFB with 2,5-Di-tert-butyl-1,4-bis(2-methoxyethoxy)benzene (DBBB) and 2,3,6-trimethylquinoxaline as the catholyte and anolyte, respectively [71]. The proof-of-concept static cell showed a low CE (70%) and EE (37%). In addition, the theoretical energy density was in the 12–16 Wh/L range and was limited by the low solubility of DBBB (0.4 M in propylene carbonate). Odom *et al.* assembled an all-organic flow cell that replaced DBBB with 3,7-bis(trifluoromethyl)-N-ethylphenothiazine (BCF3EPT) at the positive side [72]. BCF3EPT has a similar solubility and redox potential to DBBB. UV-vis absorption spectra measurements revealed that its radical cation was more stable than that of DBBB.

Similarly to aqueous organic systems, the solubility of insoluble species such as AQ and ferrocene are significantly improved by incorporating oligo ethylene oxide or quaternary ammonium moieties because of their strong solvation with organic solvents [36,73,74]. Even fine-tuning the molecular symmetry can dramatically change the form of redox materials. In dialkoxy-di-*tert*-butylbenzene derivatives, the redox center symmetricity is maintained to keep the electrochemical stability, while the incorporated poly ethylene oxide (PEO) chains help to improve the solubility in carbonated based polar electrolyte solutions [75]. These molecules show similar electrochemical reversibility with the redox potentials around 4.0 V vs. Li/Li^+. Owing to the asymmetric incorporation of PEO in ANL-8 and ANL-9 and corresponding additional intramolecular dipole moments in them, they have higher solubility to symmetric DBBB and ANL-10. As shown in Fig. 5b, unsymmetrical ANL-8 and ANL-9 are liquid at room temperature, while symmetrical DBBB and ANL-10 have much a lower solubility. Among them, ANL-8 appears to be the best candidate

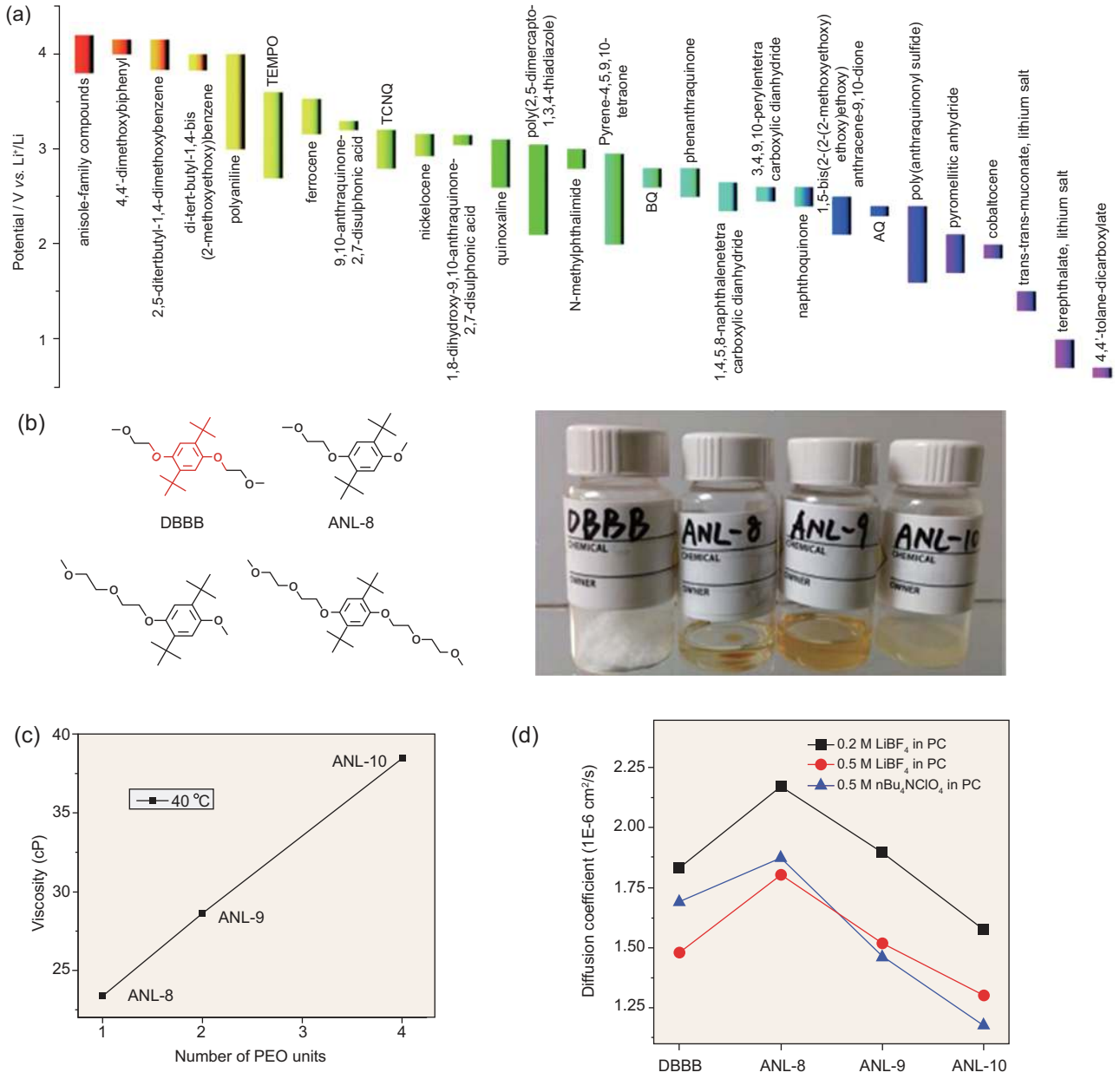

Figure 5. (a) Redox potential of representative redox-active organic and organometallic compounds with potential vs. Li/Li^+ [60] (Copyright 2015 Royal Society of Chemistry). (b) Chemical structures of picture of DBBB, ANL-8, ANL-9 and ANL-10 materials [75] (Copyright 2015 Wiley). (c) Plot of viscosity vs. PEO chain lengths of various ANL molecules [75] (Copyright 2015 Wiley). (d) Diffusion coefficient of DBBB, ANL-8, ANL-9 and ANL-10 in various electrolytes [75] (Copyright 2015 Wiley).

because of its liquid nature, higher diffusion coefficient and lower viscosity (Fig. 5c and d). Wei *et al.* coupled ANL-8 with a highly soluble anolyte compound, 9-fluorenone (FL) [76]. The cell voltage was more than 2.0 V. A microporous separator was used to enable good cell conductivity and high current operation (15 mA/cm^2, a 30-fold increase). Meanwhile, a mixed-reactant electrolyte design was adopted to mitigate crossover of active species. Figure 4c shows the typical cycling voltage curves of the flow cell using 0.5 M FL/0.5 M DMBBM/1.0 M TEA–TFSI/MeCN at the current density of 15 mA/cm^2. The flow cell achieved an EE > 70%, but was limited by continuous capacity fading. A mechanistic study revealed that the performance degradation is caused by limited chemical stability of charged radical species, especially the $FL^{\bullet -}$.

Currently, the cost of non-aqueous RFBs is still limited by several major factors. First, non-aqueous chemistries mostly use flammable solvents, which

is not ideal for large-scale applications. Some of the solvents and salts such as acetonitrile, $TFSI^-$ or PF_6^- will also significantly increase the cost. In addition, non-aqueous RFBs are normally operated at lower current densities because of lower electrolyte conductivity, which significantly affects the cell efficiency and power density, and thus increases the cost. The low current density (therefore low power) inherently leads to increased stack size, thereby affecting the overall cost.

Recent calculations have shown that all the organic-chemistry-based battery systems studied to date may not be promising for low E/P applications because the lower power densities do not allow for a small stack area. However, organic-chemistry-based systems show good promise for high E/P applications provided the concentration can be increased and divalent or more active species are used. The cost of the solvent and the active materials would still be a key factor, however. In a high E/P case of 48 hours of storage with optimistic component costs, 2 M concentration and two electrons per mol, the total cost comes to $80/kWh—a pathway to a system that costs less than the $100/kWh goal.

One possible direction for future research for both aqueous and non-aqueous redox systems could come from the experience in solid organic electrode materials for Li-ion batteries [77,78]. For inorganic materials, the redox reaction is based on the valence change of the transition-metal or elemental substance, while, for organic materials, the redox reaction is related to the charge state change of the electroactive organic group or moiety. Generally, organic materials potentially used for batteries could be divided into several groups: conjugated hydrocarbon, conjugated amine, conjugated thioether, organodisulfide, thioether, nitroxyl radical and conjugated carbonyl. Their reaction mechanisms are shown in Table 2 [78]. Among the seven types of structures, organodisulfide and conjugated carbonyl belong to *n*-type organic materials (electron transport), conjugated amine and conjugated thioether belong to *p*-type organics (hole-transport), while conjugated hydrocarbons and nitroxyl radicals belong to bipolar organic materials. A reversible redox reaction usually takes place in an organic group or moiety with conjugated structure and atoms with lone-pair electrons, such as O, N and S, because a conjugated structure is beneficial to the electron transportation and charge delocalization, and lone-pair electrons usually have a higher reaction activity.

Based on each structure listed in Table 2, the redox molecules could be rationally designed. Some basic requirements for these organic candidates include the following factors:

- Electrochemical reaction reversibility. This factor can determine cell polarization. Among the structures shown in Table 2, nitroxyl radical presents the highest reaction kinetics. On the contrary, organodisulfide and thioether show slow reaction kinetics because the bond breaking/forming of the S–S or S = O requires a high-activation energy.
- Redox potential. This factor determines the side (anode or cathode) on which the organics can be used. Generally, *p*-type organics (e.g. nitroxyl radical) have a higher redox potential than *n*-type organics (e.g. conjugated carbonyl). In addition, as discussed above for quinone-based organics, electron-withdrawing and electron-donating groups can effectively tune the redox potential.
- Solubility. Small organic molecules tend to dissolve in either aqueous or non-aqueous electrolytes. In addition, a proper substituent (e.g. hydrophilic groups for aqueous systems) or a change of structure symmetricity can effectively increase the solubility of organic materials.
- Chemical stability. This factor is very important for organic materials used in long-term applications. Degradation of some radical compounds (e.g. FL^-) is closely associated with the nature of solvents and salts. For example, FL^- fades faster in acetonitrile solvents and salts containing BF_4^- because of side reactions [76].

In addition, a lack of suitable membranes is one of the major technical hurdles impeding development of non-aqueous flow batteries. For porous separators, crossover of redox materials could cause irreversible performance degradation. Two size exclusion-based strategies have been attempted to overcome this limitation. The first strategy involves reducing the membrane pore size to increase selectivity. Helms *et al.* fabricated a porous membrane from polymers of intrinsic microporosity (PIM) with 0.8-nm pore size [79]. This PIM membrane yielded a 500-fold increase of polysulfide-blocking ability in a Li/S battery compared to Celgard (~17-nm pore). The second strategy is to put redox moieties onto polymeric backbones. Moore *et al.* demonstrated that increased size of viologen-bearing polymers greatly improves the selectivity of Celgard [80]. This method also was tried with water-soluble polymers in an aqueous flow battery [81]. However, the conductivity of PIM membranes and the solubility of redox polymers still remain a concern.

In some non-aqueous and hybrid systems, Li-ion-conducting ceramic membranes also are used; however, such membranes have limited ion conductivity and are difficult to manufacture and scale

Table 2. Structures and redox mechanisms of various types of organic materials.

Structure	Redox mechanism
Conjugated hydrocarbon	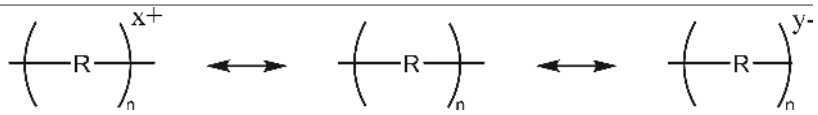
Conjugated amine	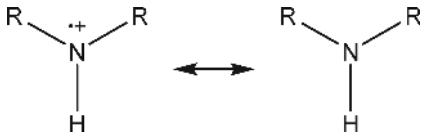
Conjugated thioether	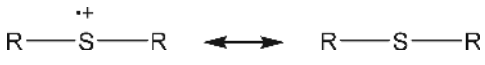
Organodisulfide	
Thioether (4e)	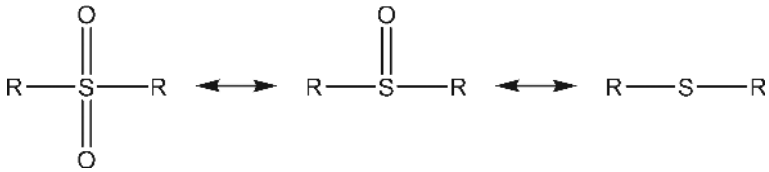
Nitroxyl radical	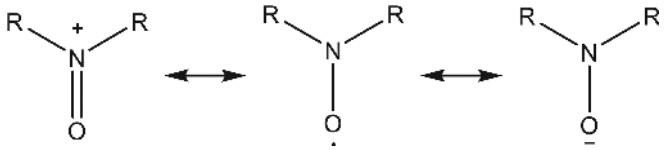
Conjugated carbonyl	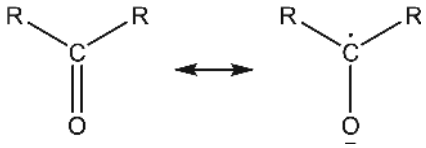

up. The high resistance across the interface between the membrane and the electrode and poor chemical compatibility also are a significant problem. The solution is likely a composite membrane or a multilayer structure that includes both ceramics and polymers. The key challenge for these alternative membranes is maintaining or improving the ionic conductivity, selectivity and chemical stability. Beyond ionic conductivity, chemical stability to redox electrolytes, physical stability in large-format cells and species selectivity are also very important. Replacing ion-exchange membranes with inexpensive porous separators can effectively reduce the total cost for both aqueous and non-aqueous systems [26,76,82,83]. Many groups have studied 'single-ion' polymers based on block copolymers, including PEO and polystyrene polymer with Li salts [84,85] and star-shaped poly(styrene)-block-poly[poly(ethylene glycol) methyl ethyl methacrylate] [86]. The basic idea is to enhance ion conductivity in the soft phase, and to improve stability in the rigid phase. To date, new commercially viable composite membranes have not emerged.

SEMI-SOLID FLOW BATTERIES

Because all redox chemistry is currently limited by the solubility of the electroactive species, Chiang's group first proposed the concept of a semi-solid RFB, enabling the RFB to be comparable to Li-ion batteries [87]. As shown in Fig. 2d [87], the particulate active materials are dispersed in the electrolyte as suspensions, essentially achieving 'infinite solubility' compared to traditional redox solutions. To achieve electronic charge transfer between the active material particles and the current collector, the active materials and conductive additives (carbon) were dispersed in a typical Li-ion battery electrolyte solution to form a percolation nanoscale conductor network in the flowable electrode suspensions. The high 'solubility' of the active materials in the suspensions and the high cell potential lead to significant increases in energy density. For example, semi-solid $LiCoO_2/Li_4Ti_5O_{12}$ produced an average 2.35-V discharge voltage with 397 Wh/L of theoretical energy density. Figure 4d shows the charge/discharge curves of this full cell. This concept was extended to a Li/S flow battery to fully use sulfur species in

the regime of Li_2S–Li_2S_8 and reach a high energy density [88], unlike Li/S flow batteries in traditional configurations that rely only on soluble polysulfides (Li_2S_4–Li_2S_8) in non-aqueous electrolytes [42,43]. Yang *et al.* constructed a metal-free, all-organic, semi-solid flow cell. They used polythiophene microparticles as both anolyte and catholyte active couples with a cell potential of 2.5 V. The active polythiophene microparticles were dispersed in 1 M $TEABF_4$–PC solution and circulated through the flow cell. It showed stable charge/discharge performance, with a high EE of 60.9% at 0.5 mA/cm^2 [89]. Similarly to a Li-ion battery, Ventosa *et al.* reported proof-of-concept for a non-aqueous, semi-solid flow battery based on Na-ion chemistry using P2-type $Na_xNi_{0.22}Co_{0.11}Mn_{0.66}O_2$ and $NaTi_2(PO_4)_3$ as positive and negative electrodes, respectively, although the energy density of the cell was around 9 Wh/L [90].

Similarly to the traditional RFB, the E/P ratio can be tuned in the design of a semi-solid flow battery to reduce the cost. In addition, low-cost active materials in powder form and low-cost carbon-conductive materials can be used. The battery-manufacturing approach can be similar to RFBs, which can be very different from the manufacturing approach for traditional Li-ion batteries [91]. A typical lithium-ion battery-manufacturing process starts with metal foil, and then layers liquid 'ink or paint' on it to form its electrodes; these steps are followed by drying and calendering. These processes need to be conducted in dry rooms or protected atmospheres. However, for a semi-solid flow battery, the manufacturing process can be simplified with the focus on preparation of semi-solid flowable inks. The cost of semi-solid flow systems was predicted to be less than 50% of that of Li-ion battery and could be less than $100/kWh [91].

The semi-solid flow battery still needs to be carefully engineered and optimized. Scale-up of the system could still be difficult. Current RFBs depend on multiple reaction stacks to increase the energy and power capacity. In a semi-solid system, the electrolyte (i.e. a suspension) needs to be conductive enough to transfer the electrons. Conductive electrolyte systems cannot be used in multiple stacks because of the shunt current through the electrolyte connecting multiple series-connected cells in a stack driven by the voltage difference between the cells. In addition, the chemistry and the physical properties of the suspension need to be carefully controlled. A high solid loading is normally desired to achieve high energy, but the high suspension viscosity could contribute to pumping-related energy losses. As a result, it is necessary to operate in either stoichiometric or intermittent flow mode. It has been suggested that either of these operating modes is capable of reducing pumping energy loss to <1% [92].

In traditional Li-ion batteries, performance depends on the formation of stable solid electrolyte interphase layers on the solid electrode materials [93]. Such stable interfaces and interphases may not exist in semi-flow battery configurations. The long-term stability of the electrode materials and the efficiency of such systems need to be carefully evaluated.

PROSPECTIVE

Overall, discussions so far suggest that aqueous redox batteries with highly soluble, low-cost materials have potential for ultra-low-cost solutions. The aqueous system is also a safer option. In 2014, the DOE released the Energy Storage Safety Strategic Plan [94]. Validation of energy-storage safety and reliability has attracted significant attention. Several safety concerns should be addressed, such as release of the stored energy during an incident, cascading failure of battery cells, fires, etc. Therefore, an aqueous flow battery is a prime candidate because of its safety, reliability and low cost. Redox materials, such as highly soluble iodine, polysulfide and all-organic materials, have demonstrated that low-cost, aqueous redox batteries also can achieve high energy or high power. Still, in these studies, stable and optimized redox couples have not been demonstrated for practical battery applications.

In addition, there is great potential in rational design of organic redox couples based on lessons from solid-state polymer electrode materials through systematically tuning the redox potential, conductivity, stability and solubility for both aqueous and non-aqueous systems. Hybrid battery designs involving either metal anodes or particulate suspensions should be investigated further. Such hybrid concepts begin to blur the boundary between traditional batteries (e.g. Li-ion battery) and RFBs, but the metal anode must be protected to prevent the metal from reacting with the electrolyte or forming dendrites [95].

There also are some non-traditional chemistries and technologies that appear to have potential to compete with Li-ion batteries in terms of energy density [96]. A very careful examination revealed that the electrolyte actively participated in electrochemical reactions in these systems. In this case, energy density is not entirely determined by the capacity of the solid-state electrode materials. Rather, it can be dictated by the concentrations of the redox species in the electrolytes. Therefore, such non-traditional chemistries actually behave more like the redox batteries we have discussed in this article. The

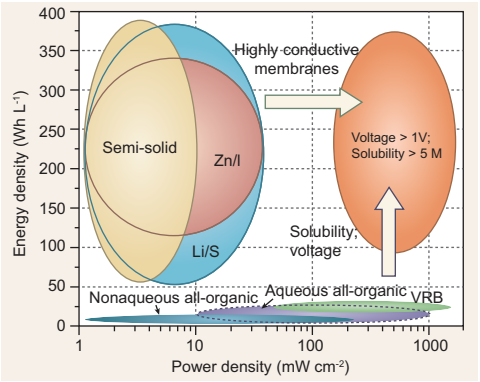

Figure 6. Energy density vs. power density for different types of RFB systems discussed in this article.

importance of solution chemistry also may apply to some other battery systems of interest, such as aqueous zinc-manganese rechargeable batteries [97–99]. The aqueous zinc-manganese system is particularly attractive because it uses some of the most abundantly available materials. The crossover between traditional batteries and RFBs and lessons learned from controlling reactions in the electrolytes have great potential to contribute to development of the ultra-low-cost technologies for the future.

As a summary, for a promising flow battery system, the primary considerations are an EE as high as possible and negligible capacity decay, which might be caused by crossover of active species through membranes or chemically unstable active species. In addition, high energy densities and power densities must be achieved to reduce the cost. Figure 6 shows energy densities and power densities of the different types of flow battery systems discussed in this article. There are two important categories of technologies: hybrid and semi-solid designs. These designs can possess high energy densities, but they suffer from low power output due to large cell resistances. The main challenge is to develop highly conductive membranes that are needed for high power output. On the other hand, although high power density can be attained in all-liquid designs, their energy densities are usually limited by low solubility of active species and cell voltage. Consequently, efforts should focus on finding low-cost, active redox couples with high solubility and cell voltages. In this regard, a highly soluble, low-cost aqueous system is the most attractive approach.

ACKNOWLEDGEMENTS

We would like to thank Drs. Vilayanur V. Viswanathan, Zimin Nie, Xiaoliang Wei, Wei Wang, David Reed and Vincent L. Sprenkle for their contribution to this manuscript.

FUNDING

The work was supported by the US Department of Energy (DOE)'s Office of Electricity Delivery and Energy Reliability (57558) for the redox-flow battery research conducted at Pacific Northwest National Laboratory. The work was also supported by the DOE Office of Basic Energy Sciences, Division of Materials Sciences and Engineering under Award (KC020105-FWP12152) for developing and organizing this manuscript. Pacific Northwest National Laboratory is a multi-program national laboratory operated by Battelle for the DOE under Contract DE-AC05-76RL01830.

REFERENCES

1. Administration, USEI. Annual Energy Review 2009.
2. van der Hoeven M. *World Energy Outlook*. Paris: International Energy Agency, 2014.
3. Osiak M, Geaney H and Armstrong E *et al.* Structuring materials for lithium-ion batteries: advancements in nanomaterial structure, composition, and defined assembly on cell performance. *J Mater Chem A* 2014; **2**: 9433–60.
4. Ferreira HL, Garde R and Fulli G *et al.* Characterisation of electrical energy storage technologies. *Energy* 2013; **53**: 288–98.
5. Dunn B, Kamath H and Tarascon J-M. Electrical energy storage for the grid: a battery of choices. *Science* 2011; **334**: 928–35.
6. Pillot C. *The Rechargeable Battery Market and main Trends 2014–2015.* http://www.avicenne.com/pdf/Fort_Lauderdale_Tutorial_C_Pillot_March2015.pdf (16 January 2017, date last accessed).
7. Li L, Kim S and Wang W *et al.* A stable vanadium redox-flow battery with high energy density for large-scale energy storage. *Adv Energy Mater* 2011; **1**: 394–400.
8. Viswanathan V, Crawford A and Stephenson D *et al.* Cost and performance model for redox flow batteries. *J Power Sources* 2014; **247**: 1040–51.
9. Lu L, Han X and Li J *et al.* A review on the key issues for lithium-ion battery management in electric vehicles. *J Power Sources* 2013; **226**: 272–88.
10. Anderman M. *Tesla Motors: Battery Technology, Analysis of the Gigafactory, and the Automakers' Perspectives.* Oregon House, CA; Total Battery Consulting, 2014.
11. Darling RM, Gallagher KG and Kowalski JA *et al.* Pathways to low-cost electrochemical energy storage: a comparison of aqueous and nonaqueous flow batteries. *Energ Environ Sci* 2014; **7**: 3459–77.
12. Ha S and Gallagher KG. Estimating the system price of redox flow batteries for grid storage. *J Power Sources* 2015; **296**: 122–32.
13. Energy USDo. *Grid Energy Storage Strategy.* 2013.
14. www.beck-elektronik.de/uploads/media/lithium-ion-vs-lead-acid.pdf (16 January 2017, date last accessed).
15. *The Prices of Batteries.* http://www.technologyreview.com/sites/default/files/legacy/jan11_feature_electric_cars_p61.pdf (16 January 2017, date last accessed).

16. Grid-Scale Rampable Intermittent Dispatchable Storage ARPA-E Funding Opportunity Announcement. Washington, DC. 2010.
17. Rastler D. *Market Driven Distributed Energy Storage System Requirements for Load Management Applications*. Palo Alto, CA: Electric Power Research Institute, 2007.
18. Zhang M, Moore M and Watson J *et al.* Capital cost sensitivity analysis of an all-vanadium redox-flow battery. *J Electrochem Soc* 2012; **159**: A1183–8.
19. Wei X, Xu W and Vijayakumar M *et al.* TEMPO-based catholyte for high-energy density nonaqueous redox flow batteries. *Adv Mater* 2014; **26**: 7649–53.
20. Cho KT, Albertus P and Battaglia V *et al.* Optimization and analysis of high-power hydrogen/bromine-flow batteries for grid-scale energy storage. *Energy Technol* 2013; **1**: 596–608.
21. Braff WA, Bazant MZ and Buie CR. Membrane-less hydrogen bromine flow battery. *Nat Commun* 2013; **4**: 2346.
22. Yang Z, Zhang J and Kintner-Meyer MC *et al.* Electrochemical energy storage for green grid. *Chem Rev* 2011; **111**: 3577–613.
23. Thaller LH. *Electrically Rechargeable Redox Flow Cells*. NASA TM X-71540. Cleveland, Ohio: National Aeronautics and Space Administration, 1974.
24. Wang W, Kim S and Chen B *et al.* A new redox flow battery using Fe/V redox couples in chloride supporting electrolyte. *Energ Environ Sci* 2011; **4**: 4068–73.
25. Lopezatalaya M, Codina G and Perez JR *et al.* Behavior of the Cr(III)/Cr(II) reaction on gold graphite-electrodes: application to redox flow storage cell. *J Power Sources* 1991; **35**: 225–34.
26. Wang W, Nie Z and Chen B *et al.* A new Fe/V redox flow battery using a sulfuric/chloric mixed-acid supporting electrolyte. *Adv Energy Mater* 2012; **2**: 487–93.
27. Skyllas-kazacos M, Rychcik M and Robins RG *et al.* New all-vanadium redox flow cell. *J Electrochem Soc* 1986; **133**: 1057–8.
28. Eckroad S. Vanadium redox flow batteries: an in-depth analysis. Palo Alto, CA: Electric Power Research Institute, 2007, 1014836.
29. Rahman F and Skyllas-Kazacos M. Vanadium redox battery: positive half-cell electrolyte studies. *J Power Sources* 2009; **189**: 1212–9.
30. Rahman F and Skyllas-Kazacos M. Solubility of vanadyl sulfate in concentrated sulfuric acid solutions. *J Power Sources* 1998; **72**: 105–10.
31. Kazacos M, Cheng M and Skyllas-Kazacos M. Vanadium redox cell electrolyte optimization studies. *J Appl Electrochem* 1990; **20**: 463–7.
32. Eric Wesoff and John JS. *Largest Capacity Flow Battery in North America and EU Is On-Line and Commissioned*. http://www.greentechmedia.com/articles/read/Largest-Capacity-Flow-Battery-in-North-America-and-EU-is-Online-and-Commiss (16 January 2017, date last accessed).
33. Haile SM. Fuel cell materials and components. *Acta Mater* 2003; **51**: 5981–6000.
34. Peighambardoust SJ, Rowshanzamir S and Amjadi M. Review of the proton exchange membranes for fuel cell applications. *Int J Hydrogen Energy* 2010; **35**: 9349–84.
35. Rikukawa M and Sanui K. Proton-conducting polymer electrolyte membranes based on hydrocarbon polymers. *Prog Polym Sci* 2000; **25**: 1463–502.
36. Wei X, Cosimbescu L and Xu W *et al.* Towards high-performance nonaqueous redox flow electrolyte via ionic modification of active species. *Adv Energy Mater* 2015; **5**: 1400678.
37. Li B, Nie Z and Vijayakumar M *et al.* Ambipolar zinc-polyiodide electrolyte for a high-energy density aqueous redox flow battery. *Nat Commun* 2015; **6**: 6303.
38. Li X, Ponce de Leon C and Walsh F *et al.* Zinc-based flow batteries for medium- and large-scale energy storage. In: Menictas C, Skyllas-Kazacos M and Lim TM (eds). *Advances in Batteries for Medium and Large-Scale Energy Storage*, 1st edn, Types and Applications. Cambridge, GB, Woodhead Publishing, 2015, 293–315.
39. Weber AZ, Mench MM and Meyers JP *et al.* Redox flow batteries: a review. *J Appl Electrochem* 2011; **41**: 1137–64.
40. Lu Y and Goodenough JB. Rechargeable alkali-ion cathode-flow battery. *J Mater Chem* 2011; **21**: 10113–7.
41. Wang Y, Wang Y and Zhou H. A Li–liquid cathode battery based on a hybrid electrolyte. *Chem Sus Chem* 2011; **4**: 1087–90.
42. Yang Y, Zheng G and Cui Y. A membrane-free lithium/polysulfide semi-liquid battery for large-scale energy storage. *Energ Environ Sci* 2013; **6**: 1552–8.
43. Pan H, Wei X and Henderson WA *et al.* On the way toward understanding solution chemistry of lithium polysulfides for high energy Li–S redox flow batteries. *Adv Energy Mater* 2015; **5**: 1500113.
44. Li N, Weng Z and Wang Y *et al.* An aqueous dissolved polysulfide cathode for lithium–sulfur batteries. *Energ Environ Sci* 2014; **7**: 3307–12.
45. Hock L. *Power Up*. http://www.rdmag.com/article/2015/09/power (23 January 2016, date last accessed).
46. Visco SJ, Nimon YS and Katz BD *et al.* Aqueous electrolyte lithium sulfur batteries. US Patent 8, 828,575, 2014.
47. Licht S. Aqueous solubilities, solubility products and standard oxidation-reduction potentials of the metal sulfides. *J Electrochem Soc* 1988; **135**: 2971–5.
48. Lu Y, Goodenough JB and Kim Y. Aqueous cathode for next-generation alkali-ion batteries. *J Am Chem Soc* 2011; **133**: 5756–9.
49. Zhao Y, Wang L and Byon HR. High-performance rechargeable lithium-iodine batteries using triiodide/iodide redox couples in an aqueous cathode. *Nat Commun* 2013; **4**: 1896.
50. Zhao Y, Ding Y and Song J *et al.* A reversible Br_2/Br— redox couple in the aqueous phase as a high-performance catholyte for alkali-ion batteries. *Energ Environ Sci* 2014; **7**: 1990–5.
51. Huskinson B, Marshak MP and Suh C *et al.* A metal-free organic-inorganic aqueous flow battery. *Nature* 2014; **505**: 195–8.
52. Yang B, Hoober-Burkhardt L and Wang F *et al.* An inexpensive aqueous flow battery for large-scale electrical energy storage based on water-soluble organic redox couples. *J Electrochem Soc* 2014; **161**: A1371–A80.
53. Chen Q, Gerhardt MR and Hartle L *et al.* A quinone-bromide flow battery with 1 W/cm^2 power density. *J Electrochem Soc* 2016; **163**: A5010–3.
54. Chen Q, Eisenach L and Aziz MJ. Cycling analysis of a quinone-bromide redox flow battery. *J Electrochem Soc* 2016; **163**: A5057–A63.
55. Er S, Suh C and Marshak MP *et al.* Computational design of molecules for an all-quinone redox flow battery. *Chem Sci* 2015; **6**: 885–93.
56. Kaixiang Lin, Chen Qing and Michael R. Gerhardt *et al.* Alkaline quinone flow battery. *Science* 2015; **349**: 1529–32.
57. Lin K, Gómez-Bombarelli R and Beh ES *et al.* A redox-flow battery with an alloxazine-based organic electrolyte. *Nat Energy* 2016; **1**: 16102.
58. Liu T, Wei X and Nie Z *et al.* A total organic aqueous redox flow battery employing low cost and sustainable methyl viologen (MV) anolyte and 4-HO-TEMPO catholyte. *Adv Energy Mater* 2016; **6**: 1501449.
59. Janoschka T, Martin N and Martin U *et al.* An aqueous, polymer-based redox-flow battery using non-corrosive, safe, and low-cost materials. *Nature* 2015; **527**: 78–81.

60. Zhao Y, Ding Y and Li Y *et al.* A chemistry and material perspective on lithium redox flow batteries towards high-density electrical energy storage. *Chem Soc Rev* 2015; **44**: 7968–96.
61. Matsuda Y, Tanaka K and Okada M *et al.* A rechargeable redox battery utilizing ruthenium complexes with non-aqueous organic electrolyte. *J Appl Electrochem* 1988; **18**: 909–14.
62. Sleightholme AE, Shinkle AA and Liu Q *et al.* Non-aqueous manganese acetylacetonate electrolyte for redox flow batteries. *J Power Sources* 2011; **196**: 5742–5.
63. Liu Q, Shinkle AA and Li Y *et al.* Non-aqueous chromium acetylacetonate electrolyte for redox flow batteries. *Electrochem Commun* 2010; **12**: 1634–7.
64. Liu Q, Sleightholme AE and Shinkle AA *et al.* Non-aqueous vanadium acetylacetonate electrolyte for redox flow batteries. *Electrochem Commun* 2009; **11**: 2312–5.
65. Mun J, Lee M-J and Park J-W *et al.* Non-aqueous redox flow batteries with nickel and iron tris (2, 2′-bipyridine) complex electrolyte. *Electrochem Solid St* 2012; **15**: A80–2.
66. Xing X, Zhao Y and Li Y. A non-aqueous redox flow battery based on tris (1,10-phenanthroline) complexes of iron (II) and cobalt (II). *J Power Sources* 2015; **293**: 778–83.
67. Zhang D, Lan H and Li Y. The application of a non-aqueous bis (acetylacetone) ethylenediamine cobalt electrolyte in redox flow battery. *J Power Sources* 2012; **217**: 199–203.
68. Suttil JA, Kucharyson JF and Escalante-Garcia IL *et al.* Metal acetylacetonate complexes for high energy density non-aqueous redox flow batteries. *J Mater Chem A* 2015; **3**: 7929–38.
69. Cappillino PJ, Pratt HD and Hudak NS *et al.* Application of redox non-innocent ligands to non-aqueous flow battery electrolytes. *Adv Energy Mater* 2014; **4:** 152–4.
70. Li Z, Li S and Liu S *et al.* Electrochemical properties of an all-organic redox flow battery using 2,2,6,6-tetramethyl-1-piperidinyloxy and N-methylphthalimide. *Electrochem Solid St* 2011; **14**: A171–3.
71. Brushett FR, Vaughey JT and Jansen AN. An all-organic non-aqueous lithium-ion redox flow battery. *Adv Energy Mater* 2012; **2**: 1390–6.
72. Kaur AP, Holubowitch NE and Ergun S *et al.* A highly soluble organic catholyte for non-aqueous redox flow batteries. *Energy Technol* 2015; **3**: 476–80.
73. Cosimbescu L, Wei X and Vijayakumar M *et al.* Anion-tunable properties and electrochemical performance of functionalized ferrocene compounds. *Sci Rep-Uk* 2015; accepted.
74. Wang W, Xu W and Cosimbescu L *et al.* Anthraquinone with tailored structure for a nonaqueous metal-organic redox flow battery. *Chem Commun* 2012; **48**: 6669–71.
75. Huang J, Cheng L and Assary RS *et al.* Liquid catholyte molecules for nonaqueous redox flow batteries. *Adv Energy Mater* 2015; **5**: 1401782.
76. Wei X, Xu W and Huang J *et al.* Radical compatibility with nonaqueous electrolytes and its impact on an all-organic redox flow battery. *Angew Chem Int Edit* 2015; **54**: 8684–7.
77. Liang Y, Tao Z and Chen J. Organic electrode materials for rechargeable lithium batteries. *Adv Energy Mater* 2012; **2**: 742–69.
78. Song Z and Zhou H. Towards sustainable and versatile energy storage devices: an overview of organic electrode materials. *Energ Environ Sci* 2013; **6**: 2280–301.
79. Li CY, Ward AL and Doris SE *et al.* Polysulfide-blocking microporous polymer membrane tailored for hybrid Li-sulfur flow batteries. *Nano Lett* 2015; **15**: 5724–9.
80. Nagarjuna G, Hui JS and Cheng KJ *et al.* Impact of redox-active polymer molecular weight on the electrochemical properties and transport across porous separators in nonaqueous solvents. *J Am Chem Soc* 2014; **136**: 16309–16.
81. Janoschka T, Martin N and Martin U *et al.* An aqueous, polymer-based redox-flow battery using non-corrosive, safe, and low-cost materials. *Nature* 2015; **527**: 78–81.
82. Zhang H, Zhang H and Li X *et al.* Nanofiltration (NF) membranes: the next generation separators for all vanadium redox flow batteries (VRBs)? *Energ Environ Sci* 2011; **4**: 1676–9.
83. Li X, Zhang H and Mai Z *et al.* Ion exchange membranes for vanadium redox flow battery (VRB) applications. *Energ Environ Sci* 2011; **4**: 1147–60.
84. Niitani T, Shimada M and Kawamura K *et al.* Synthesis of Li^+ ion conductive PEO-PSt block copolymer electrolyte with microphase separation structure. *Electrochem Solid St* 2005; **8**: A385–8.
85. Bouchet R, Maria S and Meziane R *et al.* Single-ion BAB triblock copolymers as highly efficient electrolytes for lithium-metal batteries. *Nat Mater* 2013; **12**: 452–7.
86. Niitani T, Amaike M and Nakano H *et al.* Star-shaped polymer electrolyte with microphase separation structure for all-solid-state lithium batteries. *J Electrochem Soc* 2009; **156**: A577–83.
87. Duduta M, Ho B and Wood VC *et al.* Semi-solid lithium rechargeable flow battery. *Adv Energy Mater* 2011; **1**: 511–6.
88. Fan FY, Woodford WH and Li Z *et al.* Polysulfide flow batteries enabled by percolating nanoscale conductor networks. *Nano Lett* 2014; **14**: 2210–8.
89. Oh S, Lee C-W and Chun D *et al.* A metal-free and all-organic redox flow battery with polythiophene as the electroactive species. *J Mater Chem A* 2014; **2**: 19994–8.
90. Ventosa E, Buchholz D and Klink S *et al.* Non-aqueous semi-solid flow battery based on Na-ion chemistry. P2-type $Na_xNi_{0.22}Co_{0.11}Mn_{0.66}O_2$–$NaTi_2(PO_4)_3$. *Chem Commun* 2015; **51**: 7298–301.
91. John JS. *24 M Unveils the Reinvented Lithium-Ion Battery.* http://www.greentechmedia.com/articles/read/24m-unveils-the-reinvented-lithium-ion-battery (16 January 2017, date last accessed).
92. Brunini VE. Modeling and design of semi-solid flow batteries. Doctor of Philosophy thesis, Massachusetts Institute of Technology, 2013.
93. Verma P, Maire P and Novak P. A review of the features and analyses of the solid electrolyte interphase in Li-ion batteries. *Electrochim Acta* 2010; **55**: 6332–41.
94. DOE U. *Energy Storage Safety Strategic Plan.* 2014.
95. Xu W, Wang JL and Ding F *et al.* Lithium metal anodes for rechargeable batteries. *Energ Environ Sci* 2014; **7**: 513–37.
96. Lin M-C, Gong M and Lu B *et al.* An ultrafast rechargeable aluminium-ion battery. *Nature* 2015; **27**: 3609–20.
97. Xu C, Li B and Du H *et al.* Energetic zinc ion chemistry: the rechargeable zinc ion battery. *Angew Chem Int Edit* 2012; **124**: 957–9.
98. Hertzberg B, Sviridov L and Stach EA *et al.* A manganese-doped barium carbonate cathode for alkaline batteries. *J Electrochem Soc* 2014; **161**: A835–A40.
99. Alfaruqi MH, Mathew V and Gim J *et al.* Electrochemically induced structural rransformation in a γ-MnO_2 cathode of a high capacity zinc-ion battery system. *Chem Mater* 2015; **27**: 3609–20.